Two-Dimensional Nanocrystals Produced by Exfoliation of Ti(3)AlC(2)

Michael Naguib, Murat Kurtoglu, Volker Presser, Jun Lu, Junjie Niu,
Min Heon, Lars Hultman, Yury Gogotsi and Michel W Barsoum

Submitted to ADVANCED MATERIALS

DOI: 10.1002/adma.((please add manuscript number))

Two-Dimensional Nanocrystals Produced by Exfoliation of Ti_3AlC_2

By *Michael Naguib, Murat Kurtoglu, Volker Presser, Jun Lu, Junjie Niu, Min Heon, Lars Hultman, Yury Gogotsi* and Michel W. Barsoum**

[*] Prof. Michel Barsoum and Prof. Yury Gogotsi Corresponding-Authors
Department of Materials Science and Engineering, Y.G. is also a Trustee Chair Director of A.J. Drexel Nanotechnology Institute. Drexel University, Philadelphia, PA 19104 (USA)
E-mail: (barsoumw@drexel.edu and gogotsi@drexel.edu)
Michael Naguib Author-One, Murat Kurtoglu Author-Two, Dr. Volker Presser Author-Three, Dr. Junjie Niu Author-Five, Min Heon Author-Six.
Department of Materials Science and Engineering, and A.J. Drexel Nanotechnology Institute. Drexel University, Philadelphia, PA 19104 (USA)
Jun Lu Author-Four, Prof. Lars Hultman Author-Seven
Department of Physics, IFM
Linkoping University, Linkoping 58183 (Sweden)

Keywords: Nanosheets, MAX phase, Exfoliation, Carbide, Two-dimensional material

Typically two-dimensional 2-D free-standing crystals exhibit properties that differ from those of their three-dimensional, 3-D counterparts.[1] Currently, however, there are relatively few such atomically layered solids.[2, 3, 4, 5] Herein we report on 2-D nanosheets, comprised of a few Ti_3C_2 layers and conical scrolls produced by the room temperature exfoliation of Ti_3AlC_2 in hydrofluoric acid. The large elastic moduli predicted by *ab initio* simulation, and the possibility of varying their surface chemistries (herein they are terminated by hydroxyl and/or fluorine groups) render these nanosheets attractive as polymer composite fillers. Theory also predicts that their band gap can be tuned by varying the surface terminations. The good conductivity and ductility of the treated powders suggest uses in Li-ion batteries, pseudocapacitors and other electronic applications. Since Ti_3AlC_2 is a member of a 60+ group of layered ternary carbides and nitrides known as the MAX phases, this discovery opens a door to the synthesis of a large number of other 2-D crystals.

Arguably the most studied freestanding 2-D material is graphene, which was produced by mechanical exfoliation, into single-layers in 2004[1]. Some other layered materials, such as hexagonal BN,[2] transition metal oxides and hydroxides,[4] including clays,[3] have also been exfoliated into 2-D sheets. Interestingly, exfoliated MoS_2 single layers were reported as early as in 1986.[5] Graphene is finding its way to applications ranging from supercapacitor electrodes[6] to reinforcement in composites.[7] Although graphene has attracted more attention than all other 2-D materials together, its simple chemistry and the weak van der Waals bonding between layers in multi-layer structures limit its use. Complex layered structures that contain more than one element may offer new properties because they provide a larger number of compositional variables that can be tuned for achieving specific properties. Currently, the number of non-oxide materials that have been exfoliated is limited to two fairly small groups, viz. hexagonal, van der Waals bonded structures (e.g. graphene and BN) and layered metal chalcogenides (e.g. MoS_2, WS_2, etc.).[8]

It is well established that the ternary carbides and nitrides with a $M_{n+1}AX_n$ chemistry - where n = 1, 2, or 3, M is an early transition metal, A is an A-group (mostly groups 13 and 14) element, and X is C and/or N – form laminated structures with anisotropic properties.[9][10] These, so called MAX, phases are layered hexagonal (space group $P6_3/mmc$), with two formula units per unit cell (**Figure 1**a). Near close-packed M-layers are interleaved with pure A-group element layers, with the X-atoms filling the octahedral sites between the former. One of the most widely studied and promising members of this family is Ti_3AlC_2.[11, 12] (Fig. 1a). Over 60 MAX phases are currently known to exist.[9]

The $M_{n+1}X_n$ layers are chemically quite stable. By comparison, because the A-group atoms are relatively weakly bound, they are the most reactive species. For example, heating Ti_3SiC_2 in a C-rich atmosphere results in the loss of Si and the formation of TiC_x.[13] When the same compound

is placed in molten cryolite,[14] or molten Al,[15] essentially the same reaction occurs: the Si escapes and a TiC_x forms. In the case of cryolite, the vacancies that form lead to the formation of a partially ordered cubic $TiC_{0.67}$. In both cases, the high temperatures led to a structural transformation from a hexagonal to a cubic lattice and a partial loss of layering. In some cases, such as Ti_2InC, simply heating in vacuum at ≈ 800 °C, results in loss of the A-group element and TiC_x formation.[16] Removing of both the M and A elements from MAX structure by high temperature chlorination results in a porous carbon known as carbide derived carbon with useful and unique properties.[17, 18]

Mechanical deformation of the MAX phases – which is mediated by basal dislocations and is quite anisotropic - can lead to partial delamination and formation of lamellas with thicknesses that range from tens to hundreds of nanometers.[19] However, none of MAX phases has ever been exfoliated into a few nanometer thick, crystalline layers reminiscent of graphene. Furthermore, as far as we are aware, there are no reports on the selective room, or even moderate, temperature liquid or gas phase extraction - of the A-group layers from the MAX phases and/or their exfoliation. Herein we report the extraction of the Al from Ti_3AlC_2, and formation of a new of 2-D material (Figs. 1b and c) that we propose to call "MXene" to emphasize its graphene-like morphology.

Based on the results presented below it is reasonable to conclude that the following simplified reactions occur when Ti_3AlC_2 is immersed in HF:

$$Ti_3AlC_2 + 3HF = AlF_3 + 3/2\ H_2 + Ti_3C_2 \quad (1)$$

$$Ti_3C_2 + 2H_2O = Ti_3C_2(OH)_2 + H_2 \quad (2)$$

$$Ti_3C_2 + 2HF = Ti_3C_2F_2 + H_2 \quad (3)$$

Reaction (1) is essential and is followed by reaction (2) and/or (3). In the remainder of this paper we present evidence for the aforementioned reactions and that they result in the exfoliation of 2-

D Ti_3C_2 layers, with OH and/or F surface groups (Figs. 1b and c). Reactions (2) and (3) are simplified in that they assume the terminations are OH or F, respectively, when in fact they most probably are a combination of both.

XRD spectra of the initial Ti_2AlC-TiC mixture after heating to 1350°C for 2 h resulted in peaks that corresponded mainly to Ti_3AlC_2 (bottom curve in **Fig. 2**a). When the Ti_3AlC_2 powders were placed into the HF solution, bubbles, presumed to be H_2, were observed suggesting a chemical reaction. Ultrasonication of the reaction products in methanol for 300 s resulted in significant weakening of the peaks and the appearance of an amorphous broad band around 24° (top spectrum in Fig. 2a). In other words, exfoliation leads to a loss of diffraction signal in the out-of-plane direction, and the non-planar shape of the nanosheets results in broadening of peaks corresponding to in-plane diffraction. When the same powders were cold pressed at 1 GPa, into free-standing, 300 μm thick and 25 mm diameter discs (Fig. 2e), their XRD showed that most of the non-basal plane peaks of Ti_3AlC_2 - most notably the most intense peak at ≈ 39° - disappear (middle curve in Fig. 2a). On the other hand, the (00l) peaks, such as the (002), (004) and (0010), broadened, lost intensity, and shifted to lower angles compared to their location before treatment. Using the Scherrer formula[20] the average particle dimension in the [000l] direction after treatment is estimated to be 11±3nm, which corresponds to roughly ten $Ti_3C_2(OH)_2$ layers. To identify the peaks we simulated XRD patterns of hydroxylated, viz. $Ti_3C_2(OH)_2$, (red curve in center of Fig. 2a) and fluorinated, $Ti_3C_2F_2$, structures (gold curve in center of Fig. 2a). Clearly, both were in good agreement with the XRD patterns of the pressed sample (purple curve in Fig. 2a), the agreement was better with the former. The disappearance of the most intense diffraction peak of Ti_3AlC_2 at 39° and the good agreement between the simulated XRD spectra for $Ti_3C_2(OH)_2$ and the experimental results provides strong evidence of the formation of the latter. The presence of OH groups after treatment was confirmed by FTIR.

Further DFT geometry optimization of the hydroxylated (Fig. 3f) and fluorinated structure resulted in 5% and 16% expansion of the original Ti_3AlC_2 lattice, respectively, as observed. If Al were simply removed, and not replaced by functional groups, the DFT optimization caused the structure to contract by 19 %, which is not observed. The increase of the c-lattice parameters upon reaction (Fig. 2a) is thus strong evidence for the validity of reactions 2, 3.

Raman spectra of Ti_3AlC_2, before and after HF treatment, are shown in Fig. 2b. Peaks II, III, and IV vanished after treatment, while peaks VI and VII, merged, broadened and downshifted. Such downshifting has been observed in Raman spectra of very thin layers of inorganic layered compounds.[21] The line broadening, and the spectral shifts in the Raman spectra are consistent with exfoliation and are in agreement with the broadened XRD profiles. In analogy with Ti_3SiC_2,[22] peaks I to III in Fig. 2b can be assigned to Al-Ti vibrations, while peaks V and VI involve only Ti-C vibrations. The fact that only the latter two exist after etching confirms both the mode assignments, but more importantly the loss of Al from the structure. Note that peaks V and VI are combined, broadened and downshifted.

The Ti 2p XPS spectra, before and after treatment, are shown in Fig. 2c. The C 1s and Ti 2p peaks before treatment match previous work on Ti_3AlC_2.[23] The presence of Ti-C and Ti-O bonds was evident from both spectra, indicating the formation of $Ti_3C_2(OH)_2$ after treatment. The Al and F peaks (not shown) were also observed and their concentrations were calculated to be around 3 at.% and 12 at.%, respectively. Aluminum fluoride (AlF_3) – a reaction product, see below - can probably account for most of the F signal seen in the spectra. The O 1s main signal (not shown at ~530.3 cm^{-1}) suggest the presence of OH group.[24]

A SEM image of a ≈ 1500 μm^3 Ti_3AlC_2 particle (Fig. 2d) shows how the basal planes fan out and spread apart as a result of the HF treatment. EDAX of the particles showed them to be comprised of Ti, C, O and F, with little, or no, Al. This implies that the Al layers were replaced

by oxygen (i.e. OH) and/or F. Note that the exfoliated particles maintained the pseudo-ductility of Ti_3AlC_2 and could be easily CP into freestanding disks (Fig. 2e). This property can prove crucial in some potential applications, such as anodes for Li-ion batteries.

TEM analysis of exfoliated sheets (**Fig. 3**a,b) shows them to be quite thin and transparent to electrons since the carbon grid is clearly seen below them. This fact strongly suggests a very thin foil, especially considering the high atomic number of Ti. The corresponding selected area diffraction, SAD (inset in Fig. 3b) shows the hexagonal symmetry of the basal planes. EDAX of the same flake showed the presence of Ti, C, O, and F. Figures 3c,d show cross-sections of exfoliated single- and double-layer MXene sheets. Figures 3e,f show high-resolution TEM micrographs and a simulated structure of two adjacent OH-terminated Ti_3C_2 sheets, respectively. The experimentally observed interplanar distances and angles are found to be in good agreement with the calculated structure. **Figures 4**a,b show stacked multilayer MXene sheets. The exfoliated layers can apparently also be rolled into conical shapes (Fig. 4d); some are bent to radii of < 20 nm (Fig. 4e). Note that if Al atoms had been replaced by C atoms, the concomitant formation of strong Ti-C bonds - as when, for example, Ti_3SiC_2 reacts with cryolite at 900 °C- [14] exfoliation would not have been possible. It follows that the reaction must have resulted in a solid in which the Ti-Al bonds are replaced by much weaker hydrogen or van der Waals bonds. This comment notwithstanding, the EDAX results consistently show the presence of F in the reaction products implying that, as noted above, the terminations are most likely a mixture of F and OH. The presence of up to 12 at.% F has also been confirmed using XPS. In the latter case, however, some of it could originate from AlF_3 residue in the sample.

Lastly, it is instructive to point out the similarities between MXene and graphene such as, i) the exfoliation of 2-D Ti_3C_2 layers (Figs. 4a and b) into multilayer sheets that resemble exfoliated graphite,[25] ii) the formation of scrolls (Figs. 4d and e). Also, as cross-sectional TEM

(Fig. 4e) shows, some nanosheets were bent to radii < 20 nm without fracture, which is evidence for strong and flexible Ti_3C_2 layers. Similar scrolls were produced by sonication of grapheme.[26, 27] We assume that the sonication used for exfoliation caused some nanosheets to roll into scrolls, as schematically shown in Fig. 4f.

Multilayer structures may be used, for example, as hosts for Li storage. DFT calculations at 0 K and in Li-rich environments show that the formation of $Ti_3C_2Li_2$ as a result of the intercalation of Li into the space vacated by the Al atoms (Fig. 4c) assuming reaction

$$Ti_3C_2 + 2Li = Ti_3C_2Li_2 \quad (4)$$

has an enthalpy change of 0.28 eV. One possible reason for the positive value maybe the fact that Li has an atomic radius of 145 pm, whereas that of Al is 125 pm. The structure shown in Fig. 4c would provide a capacity of 320 $mAhg^{-1}$, which is comparable to the 372 $mAhg^{-1}$ of graphite for (LiC_6).

The elastic modulus of a single, exfoliated $Ti_3C_2(OH)_2$ layer, along the basal plane, is calculated to be around 300 GPa, which is within the typical range of transition metal carbides and significantly higher than most oxides and clays.[3] And while the 302 GPa value is lower than that of graphene,[7] the existence of surface functional groups for the treated powders, should ensure better bonding to and better dispersion in polymer matrices if these exfoliated layers are to be used as reinforcements in polymer composites. It is also fair to assume the bending rigidity of the Ti_3C_2 layers to be significantly higher than graphene. It is important to note here that the Ti_3C_2 sheets were much more stable than graphene sheets under the 200 kV electron beam in the TEM.

DFT calculations also predict that the electronic properties of the exfoliated layers are a function of surface termination (Fig. 3g). The calculated band structure of a single Ti_3C_2 layer resembles a typical semi-metal with a finite density of states at the Fermi level. Indeed, the

resistivity of the thin disk shown in Fig. 2e is estimated to about an order of magnitude higher than the same disc made with unreacted Ti_2AlC powders, which translates to a resistivity of ≈ 0.03 μΩm. This low resistivity should prove beneficial in applications such as Li-ion batteries (Fig. 4c) or pseudo-capacitor electrodes, replacing layered transition metal oxides,[28] which show useful red-ox properties and Li-intercalation,[29] but have low electrical conductivities. When terminated with OH and F groups, the band structure has a semiconducting character with a clear separation between valence and conduction bands by 0.05 eV and 0.1 eV, respectively (Fig. 3g). Thus, it is reasonable to assume that it would be possible to tune the electronic structure of exfoliated MAX layers by varying the functional groups. This behavior may be useful in certain electronic applications, such as transistors, where the use of graphene[30] and MoS_2[31] has been successfully demonstrated.

In conclusion, the treatment of Ti_3AlC_2 powders for 2 h in HF results in the formation exfoliated 2-D Ti_3C_2 layers. The exposed Ti surfaces appear to be terminated by OH and/or F. The implications, and importance, of this work go far beyond the results shown herein. As noted above, there are over 60 currently known MAX phases and thus this work, in principle, opens the door for formation of a large number of 2-D $M_{n+1}X_n$ structures, including the carbides *and* nitrides of Ti, V, Cr, Nb, Ta, Hf and Zr. The latter could include 2-D structures of combination of M-atoms, (e.g. $(Ti_{0.5}Zr_{0.5}InC)$[32] and/or different combination of C and N (e.g. $Ti_2AlC_{0.5}N_{0.5}$),[33] if the selective chemical etching is extended to other MAX phases. We currently have solid results for the exfoliation of Ta_4AlC_3 into Ta_4C_3 flakes.

Experimental Section

Powder of Ti_3AlC_2 was prepared by ball-milling Ti_2AlC (> 92 wt.% 3-ONE-2, Voorhees, NJ) and TiC (99% Johnson Matthey Electronic, NY) powders in a 1:1 molar ratio for 24 h using zirconia balls. The mixture was heated to 1350°C for 2 h under argon, Ar. The resulting loosely

held compact was crushed in a mortar and pestle. Roughly 10 g of powders are then immersed in ≈ 100 ml of a 50 % concentrated hydrofluoric acid, HF, (Fisher Scientific, Fair Lawn, NJ) solution at room temperature for 2 h. The resulting suspension was then washed several times using deionised water and centrifuged to separate the powders. In some cases, to align the flakes and produce free-standing discs, the treated powders were cold pressed at a load corresponding to a stress of 1 GPa in a steel die.

X-ray diffraction (XRD) patterns were obtained with a powder diffractometer (Siemens D500, Germany) using Cu K_α radiation, and a step scan of 0.02° and 1 s per step. Si powder was added to some samples as an internal standard. A scanning electron microscope, (SEM, Zeiss Supra 50VP, Germany) was used to obtain high magnification images of the treated powders. Transmission electron microscopes, TEMs, (JEOL JEM-2100F and JEM 2100, Japan; FEI, Tecnai G2 TF20UT FEG, Netherlands) operating at 200 kV were used to characterize the exfoliated powders. Chemical analysis in the TEM was carried out using an ultra-thin window X-ray energy dispersive spectrometer, EDAX (EDAX, Mahwah, NJ). The TEM samples were prepared by deposition of the flakes - from an isopropanol suspension - on a lacey-200 mesh carbon coated copper grid. Raman spectroscopy of the cold pressed samples was carried out on a microspectrometer (inVia, Renishaw plc, Gloucestershire, UK) using an Ar ion laser (514.5 nm) and a grating with 1800 lines/mm. This corresponds to a spectral resolution of 1.9 cm^{-1} and a spot size of 0.7 μm in the focal plane. X-ray photoelectron spectroscopy, XPS, (PHI 5000, ULVAC-PHI, Inc., Japan) was used to analyze the surfaces of samples before and after exfoliation.

Theoretical calculations were performed by density functional theory (DFT) using the plane-wave pseudo-potential approach, with ultrasoft pseudopotentials and Perdew Burke Ernzerhof (PBE) exchange - Wu-Cohen (WC) correlation functional, as implemented in the CASTEP code in Material Studio software (Version 4.5). A 8x8x1 Monkhorst-Pack grid and

planewave basis set cutoff of 500 eV were used for the calculations. Exfoliation was modeled by first removing Al atoms from the Ti_3AlC_2 lattice. Exposed Ti atoms located on the bottom and top of the remaining Ti_3C_2 layers were saturated by OH (Fig. 1b) or F groups followed by full geometry optimization until all components of the residual forces became less than 0.01 eV/Å. Equilibrium structures for exfoliated layers were determined by separating single Ti_3C_2 layers by a 1.2 nm thick vacuum space in a periodic supercell followed by the aforementioned full geometry optimization. Band structures of the optimized materials were calculated using a k point separation of $0.015 Å^{-1}$. The elastic properties of the 2-D structures were calculated by subjecting the optimized structure to various strains and calculating the resulting second derivatives of the energy density.

Acknowledgments:

This work was supported by the Assistant Secretary for Energy Efficiency and Renewable Energy, Office of Vehicle Technologies of the U.S. Department of Energy under Contract No. DE-AC02-05CH11231, Subcontract 6951370 under the Batteries for Advanced Transportation Technologies (BATT) Program. M. K. was supported by Gurallar Co., Turkey. V.P. was supported by Alexander von Humboldt Foundation. The authors are thankful to Dr. V. Mochalin for help with FTIR analysis. L. H. acknowledges support from the Swedish Foundation for Strategic Research, the Knut and Alice Wallenberg Foundation, a Swedish Government Strategic Grant and an European Research Council Advanced Grant.

References

[1] K. S. Novoselov, A. K. Geim, S. V. Morozov, D. Jiang, Y. Zhang, S. V. Dubonos, I. V. Grigorieva, A. A. Firsov, Science 2004, 306, 666.
[2] D. Pacilé, J. C. Meyer, C. O. Girit, A. Zettl, Applied Physics Letters 2008, 92, 133107.
[3] P. H. Nadeau, Applied Clay Science 1987, 2, 83.
[4] R. Ma, T. Sasaki, Advanced Materials 2010, 22, 5082.
[5] P. Joensen, R. F. Frindt, S. R. Morrison, Materials Research Bulletin 1986, 21, 457.
[6] M. D. Stoller, S. Park, Y. Zhu, J. An, R. S. Ruoff, Nano Letters 2008, 8, 3498.
[7] S. Stankovich, D. A. Dikin, G. H. B. Dommett, K. M. Kohlhaas, E. J. Zimney, E. A. Stach, R. D. Piner, S. T. Nguyen, R. S. Ruoff, Nature 2006, 442, 282.
[8] J. N. Coleman, M. Lotya, A. O'Neill, S. D. Bergin, P. J. King, U. Khan, K. Young, A. Gaucher, S. De, R. J. Smith, I. V. Shvets, S. K. Arora, G. Stanton, H. Y. Kim, K. Lee, G. T. Kim, G. S. Duesberg, T. Hallam, J. J. Boland, J. J. Wang, J. F. Donegan, J. C. Grunlan, G. Moriarty, A. Shmeliov, R. J. Nicholls, J. M. Perkins, E. M. Grieveson, K. Theuwissen, D. W. McComb, P. D. Nellist, V. Nicolosi, Science 2011, 331, 568.
[9] M. W. Barsoum, Progress in Solid State Chemistry 2000, 28, 201.
[10] M. W. Barsoum, in *Ceramics Science and Technology, Vol. 2: Properties,*, Vol. 2 (Eds: R. R. Riedel, I.-W. Chen), Wiley-VCH Verlag GmbH & Co, 2010.
[11] X. H. Wang, Y. C. Zhou, Journal of Materials Science & Technology 2010, 26, 385.
[12] N. V. Tzenov, M. W. Barsoum, Journal of the American Ceramic Society 2000, 83, 825.
[13] T. El-Raghy, M. W. Barsoum, J. Appl. Phys. 1998, 83, 112.
[14] M. W. Barsoum, T. El-Raghy, L. Farber, M. Amer, R. Christini, A. Adams, J. Electrochem. Soc. 1999, 146, 3919.
[15] T. El-Raghy, M. W. Barsoum, M. Sika, Mater. Sci. Eng. A 2001, **298**, 174.
[16] M. W. Barsoum, J. Golczewski, H. J. Siefert, F. Aldinger, J. Alloys and Compds. 2002, 340, 173.
[17] Y. Gogotsi, A. Nikitin, H. Ye, W. Zhou, J. E. Fischer, B. Yi, H. C. Foley, M. W. Barsoum, Nature Materials 2003, 2, 591.
[18] G. Yushin, E. N. Hoffman, M. W. Barsoum, Y. Gogotsi, C. A. Howell, S. R. Sandeman, G. J. Phillips, A. W. Lloyd, S. V. Mikhalovsky, Biomaterials 2006, 27, 5755.
[19] M. W. Barsoum, M. Radovic, in *Encyclopedia of Materials: Science and Technology*, (Eds: K. H. J. Buschow, W. C. Robert, C. F. Merton, I. Bernard, J. K. Edward, M. Subhash, V. Patrick), Elsevier, Oxford 2004, 1.
[20] B. D. Cullity, *Elements of X-ray diffraction*, Addison-Wesley 1978.
[21] C. N. R. Rao, et al., Science and Technology of Advanced Materials 2010, 11, 054502.
[22] J. Spanier, S. Gupta, M. Amer, M. W. Barsoum, Physical Review B 2005, 71, 012103.
[23] S. Myhra, J. A. A. Crossley, M. W. Barsoum, Journal of Physics and Chemistry of Solids 2001, 62, 811.
[24] M. Schmidt, S. G. Steinemann, Fresenius' Journal of Analytical Chemistry 1991, 341, 412.
[25] L. M. Viculis, J. J. Mack, O. M. Mayer, H. T. Hahn, R. B. Kaner, Journal of Materials Chemistry 2005, 15, 974.
[26] L. M. Viculis, J. J. Mack, R. B. Kaner, Science 2003, 299, 1361.
[27] M. V. Savoskin, V. N. Mochalin, A. P. Yaroshenko, N. I. Lazareva, T. E. Konstantinova, I. V. Barsukov, I. G. Prokofiev, Carbon 2007, 45, 2797.
[28] T. Brezesinski, J. Wang, S. H. Tolbert, B. Dunn, Nat Mater 2010, 9, 146.
[29] K. Kang, Y. S. Meng, J. Bréger, C. P. Grey, G. Ceder, Science 2006, 311, 977.
[30] F. Schwierz, Nat Nano 2010, 5, 487.

[31] B. Radisavljevic, A. Radenovic, J. Brivio, V. Giacometti, A. Kis, Nat Nano 2011, advance online publication.
[32] S. Gupta, E. N. Hoffman, M. W. Barsoum, Journal of Alloys and Compounds 2006, 426, 168.
[33] M. W. Barsoum, T. El-Raghy, M. Ali, Metallurgical and Materials Transactions A 2000, 31, 1857.

Figure Captions;

Figure 1. Schematic of the exfoliation process for Ti_3AlC_2. (a) Ti_3AlC_2 structure. (b) Al atoms replaced by OH after reaction with HF. (c) Breakage of the hydrogen bonds and separation of nano sheets after sonication in methanol.

Figure 2. Analysis of Ti_3AlC_2 before and after exfoliation. (a) XRD pattern for Ti_3AlC_2 before any treatment, simulated XRD patterns of $Ti_3C_2F_2$ and $Ti_3C_2(OH)_2$, measured XRD patterns of Ti_3AlC_2 after HF treatment, and exfoliated nanosheets produced by sonication. (b) Raman spectra of Ti_3AlC_2 before and after HF treatment. (c) XPS spectra of Ti_3AlC_2 before and after HF treatment. (d) SEM image of a sample after HF treatment. (e) CP 25 mm disk of etched and exfoliated material after HF treatment.

Figure 3. Exfoliated MXene nanosheets. (a) TEM micrographs of exfoliated 2-D nanosheets of Ti-C-O-F. (b) Exfoliated 2-D nanosheets; inset SAD shows hexagonal basal plane. (c) Single and double layer MXene sheets. (d) HRTEM image showing the separation of individual sheets after sonication. (e) HRTEM image of bilayer $Ti_3C_2(OH)_xF_y$. (f) Atomistic model of the layer structure shown in E. (g) Calculated band structure of single layer MXene with -OH and -F surface termination and no termination (Ti_3C_2), showing a change from metal to semiconductor as a result of change in the surface chemistry.

Figure 4. TEM images and simulated structures of multi-layer MXene. (a) TEM micrographs for stacked layers of Ti-C-O-F. Those are similar to multilayer graphene or exfoliated graphite that finds use in electrochemical storage. (b) The same as A but at a higher magnification. (c) Model of the Li-intercalated structure of Ti_3C_2 ($Ti_3C_2Li_2$) (d) Conical scroll of about 20 nm in outer diameter. (e) Cross sectional TEM image of a scroll with inner radius less than 20 nm. (f) Schematic for MXene scroll (OH-terminated).

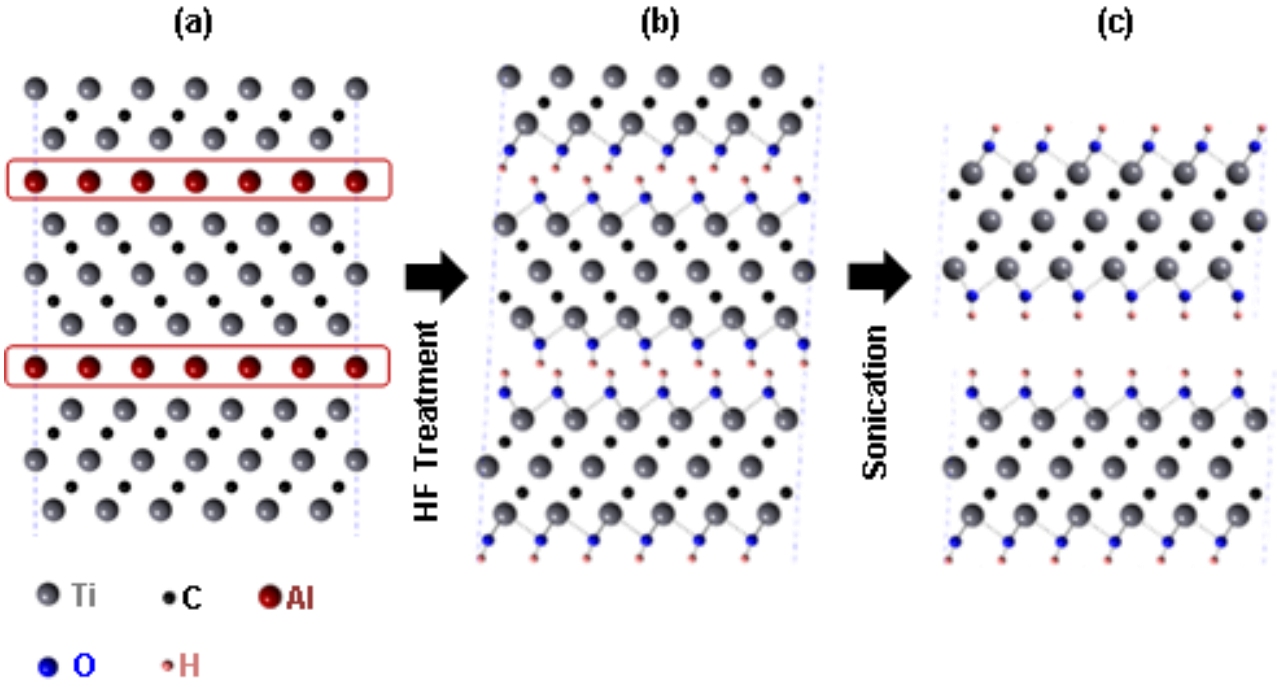

Figure 1. Schematic of the exfoliation process for Ti_3AlC_2. (a) Ti_3AlC_2 structure. (b) Al atoms replaced by OH after reaction with HF. (c) Breakage of the hydrogen bonds and separation of nano sheets after sonication in methanol.

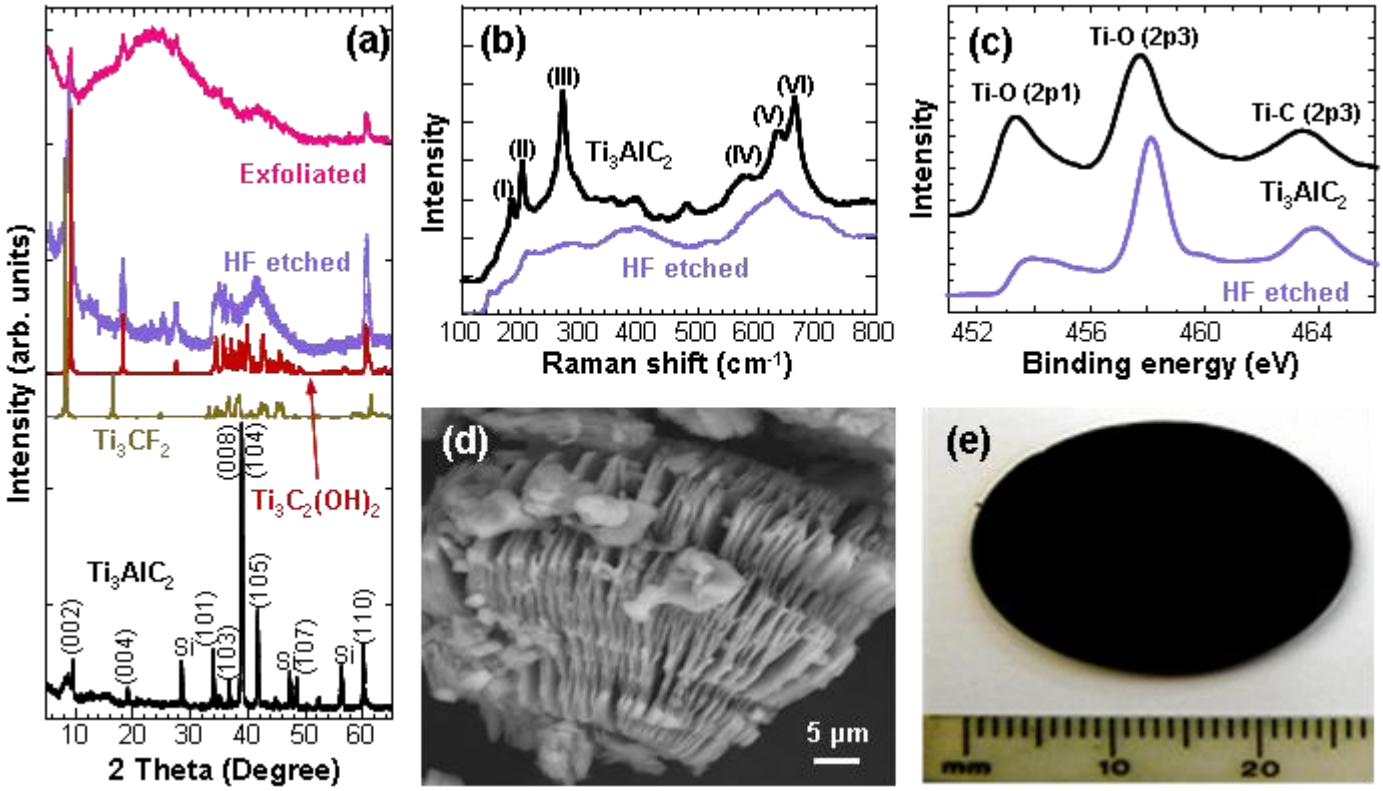

Figure 2. Analysis of Ti_3AlC_2 before and after exfoliation. (a) XRD pattern for Ti_3AlC_2 before any treatment, simulated XRD patterns of $Ti_3C_2F_2$ and $Ti_3C_2(OH)_2$, measured XRD patterns of Ti_3AlC_2 after HF treatment, and exfoliated nanosheets produced by sonication. (b) Raman spectra of Ti_3AlC_2 before and after HF treatment. (c) XPS spectra of Ti_3AlC_2 before and after HF treatment. (d) SEM image of a sample after HF treatment. (e) CP 25 mm disk of etched and exfoliated material after HF treatment.

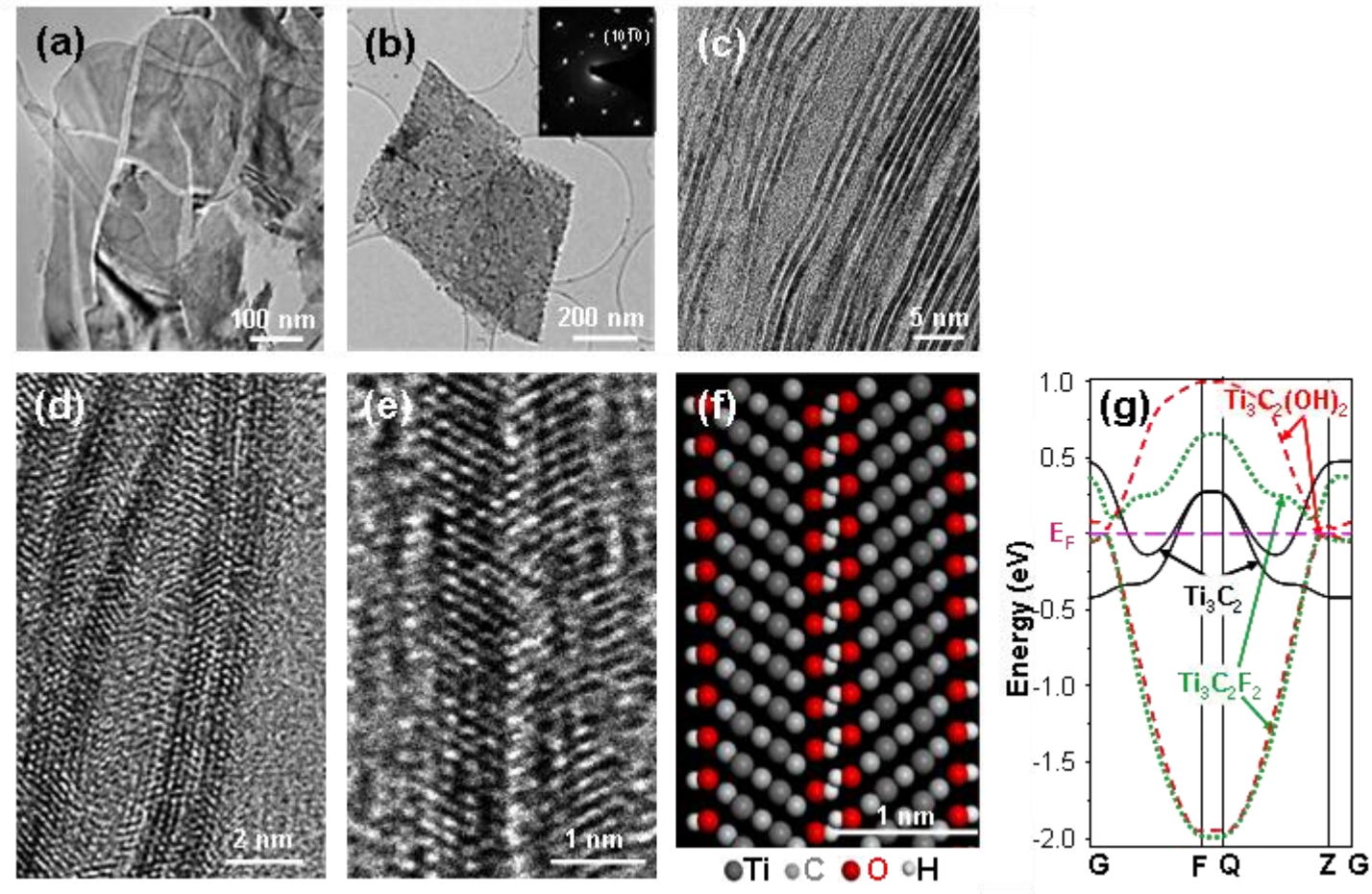

Figure 3. Exfoliated MXene nanosheets. (a) TEM micrographs of exfoliated 2-D nanosheets of Ti-C-O-F. (b) Exfoliated 2-D nanosheets; inset SAD shows hexagonal basal plane. (c) Single and double layer MXene sheets. (d) HRTEM image showing the separation of individual sheets after sonication. (e) HRTEM image of bilayer $Ti_3C_2(OH)_xF_y$. (f) Atomistic model of the layer structure shown in E. (g) Calculated band structure of single layer MXene with -OH and -F surface termination and no termination (Ti_3C_2), showing a change from metal to semiconductor as a result of change in the surface chemistry.

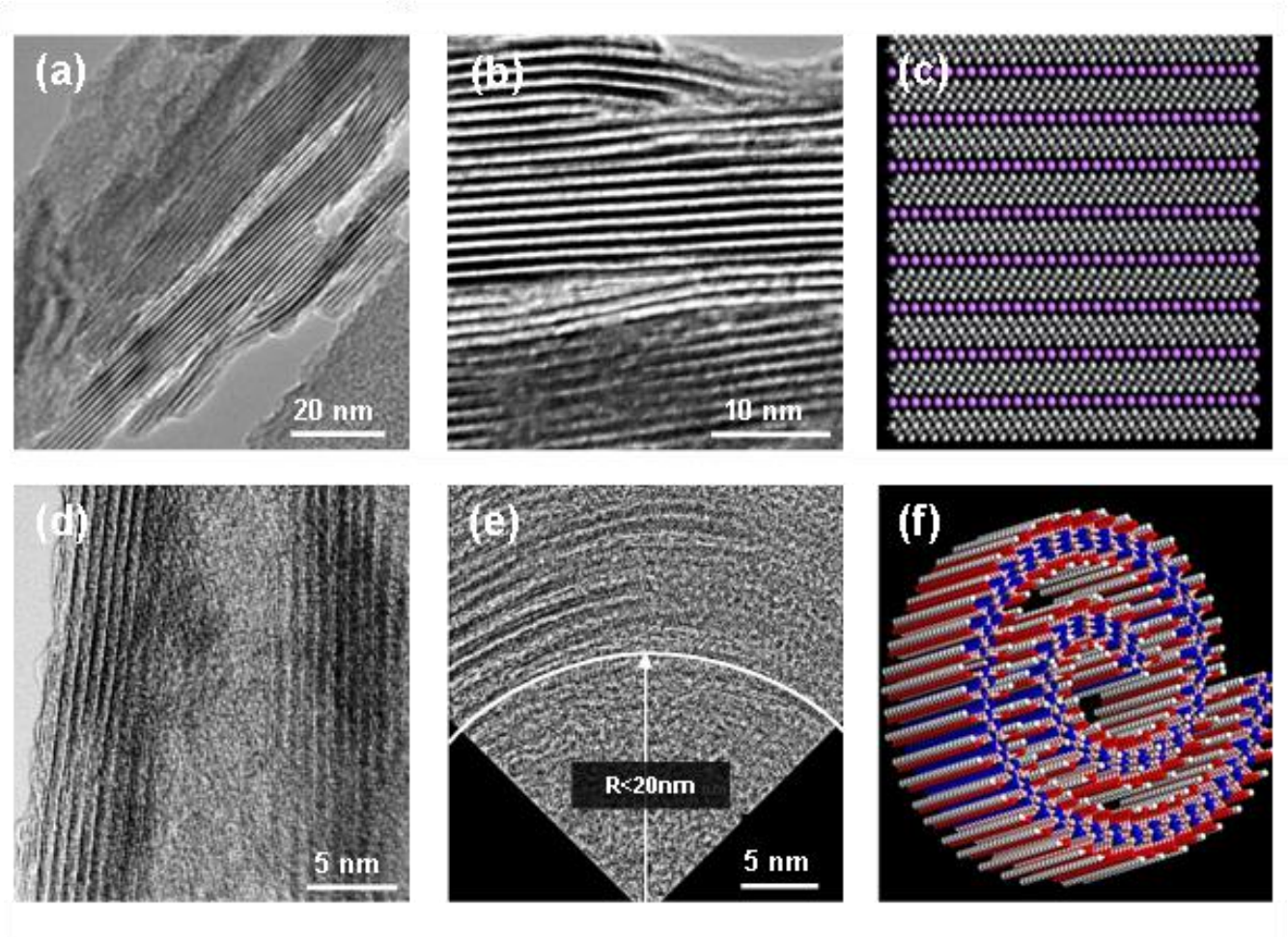

Figure 4. TEM images and simulated structures of multi-layer MXene. (a) TEM micrographs for stacked layers of Ti-C-O-F. Those are similar to multilayer graphene or exfoliated graphite that finds use in electrochemical storage. (b) The same as A but at a higher magnification. (c) Model of the Li-intercalated structure of Ti_3C_2 ($Ti_3C_2Li_2$) (d) Conical scroll of about 20 nm in outer diameter. (e) Cross sectional TEM image of a scroll with inner radius less than 20 nm. (f) Schematic for MXene scroll (OH-terminated).

Received: ((will be filled in by the editorial staff))
Revised: ((will be filled in by the editorial staff))
Published online: ((will be filled in by the editorial staff))

The table of contents entry:

Two-dimensional nanocrystals have unique properties. Herein we report on two-dimensional Ti_3C_2 nanosheets, multi-layers structures and conical scrolls produced by room temperature exfoliation of Ti_3AlC_2 in HF. Since Ti_3AlC_2 is a member of a 60+ group of layered ternary carbides and nitrides (MAX phases), this discovery opens a door to the synthesis of a large number of other 2-D crystals.

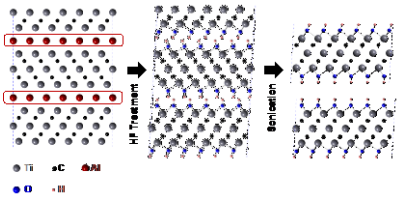

Keyword (Two-Dimensional Nanocrystals)

Michael Naguib, Murat Kurtoglu, Volker Presser, Jun Lu, Junjie Niu, Min Heon, Lars Hultman, Yury Gogotsi* and Michel W. Barsoum*

Two-Dimensional Nanocrystals Produced by Exfoliation of Ti_3AlC_2

ToC figure ((55 mm broad, 50 mm high, or 110 mm broad, 20 mm high))

Supporting Information should be included here (for submission only; for publication, please provide Supporting Information as a separate PDF file).